Inhibitory interneurons mediate autism-associated behaviors via 4E-BP2

Shane Wiebe[a,b,1], Anmol Nagpal[a,b,c,1], Vinh T. Truong[a,b], Jeehyun Park[a,b], Agnieszka Skalecka[a,b], Alexander J. He[a,b], Karine Gamache[d], Arkady Khoutorsky[e,f], Ilse Gantois[a,b,2], and Nahum Sonenberg[a,b,2,3]

[a]Department of Biochemistry, McGill University, Montreal, QC H3G 1Y6, Canada; [b]Goodman Cancer Research Centre, McGill University, Montreal, QC H3A 1A3, Canada; [c]Integrated Program in Neuroscience, Montreal Neurological Institute, McGill University, Montreal, QC H3A 2B4, Canada; [d]Department of Psychology, McGill University, Montreal, QC H3A 1B1, Canada; [e]Department of Anesthesia, McGill University, Montreal, QC H4A 3J1, Canada; and [f]Alan Edwards Centre for Research on Pain, McGill University, Montreal, QC H3A 0G1, Canada

Contributed by Nahum Sonenberg, July 22, 2019 (sent for review May 14, 2019; reviewed by Eric Klann and Frank Kooy)

Translational control plays a key role in regulation of neuronal activity and behavior. Deletion of the translational repressor 4E-BP2 in mice alters excitatory and inhibitory synaptic functions, engendering autistic-like behaviors. The contribution of 4E-BP2-dependent translational control in excitatory and inhibitory neurons and astrocytic cells to these behaviors remains unknown. To investigate this, we generated cell-type-specific conditional 4E-BP2 knockout mice and tested them for the salient features of autism, including repetitive stereotyped behaviors (self-grooming and marble burying), sociability (3-chamber social and direct social interaction tests), and communication (ultrasonic vocalizations in pups). We found that deletion of 4E-BP2 in GABAergic inhibitory neurons, defined by *Gad2*, resulted in impairments in social interaction and vocal communication. In contrast, deletion of 4E-BP2 in forebrain glutamatergic excitatory neurons, defined by *Camk2a*, or in astrocytes, defined by *Gfap*, failed to cause autistic-like behavioral abnormalities. Taken together, we provide evidence for an inhibitory-cell-specific role of 4E-BP2 in engendering autism-related behaviors.

autism | conditional knockout | interneurons | behavior | 4E-BP2

Autism spectrum disorder (ASD) is a class of heterogeneous neurodevelopmental conditions that affect ∼1% of the world population (1). The core clinical symptoms of ASD include altered sociability, impaired verbal or nonverbal communication, and repetitive or restrictive behaviors. ASD is often comorbid with anxiety, seizures, cognitive defects, and mood and sleep disorders (2). The etiology for the majority of ASD cases is unknown, but strong evidence indicates that ASD is likely caused by a complexity of genetic factors (3).

Mutations in many genes important for synaptic function can cause behavioral deficits (4). The protein landscape of a synapse is fundamental for brain function and behavior and is therefore tightly regulated. Many genes (5) and gene mutations (6) are linked to the development of ASD and can be broken into functional clusters, such as those genes regulating mRNA translation or encoding structural synaptic proteins (7, 8).

All nuclear-encoded eukaryotic mRNAs are capped at their 5′ end with a modified guanine nucleotide (m^7GpppN, where N is any nucleotide) (9). Binding of eukaryotic initiation factor 4E (eIF4E) to the 5′ cap is required to initiate translation. eIF4E is a subunit of the eIF4F complex, which also contains eIF4A, an RNA helicase, and eIF4G, a scaffolding protein (10). The formation of eIF4F is rate limited by the availability of eIF4E which is the least abundant translation initiation factor (11, 12). eIF4E binding to the mRNA 5′ cap is repressed by a family of proteins called eIF4E-binding proteins (4E-BPs) (13), consisting of 3 paralogs encoding 4E-BP1, 4E-BP2, and 4E-BP3 in mammals. 4E-BPs compete with eIF4G for a shared binding site on eIF4E, hence disrupting eIF4F complex formation (14). Phosphorylation of 4E-BPs via the mechanistic/mammalian target of rapamycin complex 1 (mTORC1) decreases their binding affinity for eIF4E and allows for enhanced eIF4F complex formation and translation initiation (15).

Aberrant cap-dependent mRNA translation is a cause of ASD (7). Mutations in the upstream regulators of mTORC1 such as tuberous sclerosis complex 1 and 2 (TSC1/2), neurofibromatosis 1, and phosphatase and tensin homolog (PTEN) (16) render the mTORC1 pathway hyperactive and cause autism-related behaviors in mice (17) and humans (18). Additionally, up-regulation of the mTOR and MAPK pathways correlate with the severity of idiopathic autism in individuals (19, 20). Downstream of mTORC1, exaggeration of eIF4E activity engenders autistic-like behaviors in mice (21, 22). Also, it was reported that 2 individuals with ASD harbored a mutation in the promoter of *EIF4E*, which renders the gene hyperactive (23). Thus, dysregulation of translation initiation constitutes an ASD risk factor.

4E-BP2 is the predominant 4E-BP paralog expressed in the brain (24). Global deletion of 4E-BP2 in mice engenders autistic-like behaviors, including reduced social interaction in the 3-chamber social and direct social interaction tests, exaggerated grooming and marble burying, and altered ultrasonic vocalizations (USVs) in pups (21). The excitatory and inhibitory synaptic activity in the hippocampus of these mice was also exaggerated, where excitation was increased to a larger extent than inhibition (21). As such, it is important to study autism-associated behaviors mediated by 4E-BP2 in excitatory versus inhibitory neurons, as well as the astrocytes controlling their activity (25, 26). To this end, we generated conditional knockout (cKO) mouse models of 4E-BP2 in excitatory (glutamatergic) neurons, inhibitory (GABAergic)

Significance

Disrupting cellular mechanisms that control protein synthesis can lead to autism spectrum disorder (ASD) in humans. Repetitive motions, impaired social interaction, and altered vocal communication are core symptoms of ASD and can be mimicked in mice. Deletion of the protein synthesis inhibitor, eukaryotic initiation factor 4E binding protein 2 (4E-BP2), causes autistic behaviors in mice. Using a variety of conditional knockout mouse models, we found that loss of 4E-BP2 in inhibitory neurons in the brain, but not in excitatory neurons or astrocytes, causes autistic behaviors.

Author contributions: S.W., A.N., A.K., I.G., and N.S. designed research; S.W., A.N., V.T.T., J.P., A.S., and A.J.H. performed research; K.G. contributed new reagents/analytic tools; S.W., A.N., V.T.T., J.P., A.S., A.J.H., and K.G. analyzed data; and S.W., A.N., I.G., and N.S. wrote the paper.

Reviewers: E.K., New York University; and F.K., University of Antwerp.

Conflict of interest statement: I.G., N.S., and F.K. were co-authors on a 2017 review article.

[1]S.W. and A.N. contributed equally to this work.

[2]I.G. and N.S. contributed equally to this work.

[3]To whom correspondence may be addressed. Email: nahum.sonenberg@mcgill.ca.

Published online August 19, 2019.

www.pnas.org/cgi/doi/10.1073/pnas.1908126116

interneurons, and astrocytes. Using behavioral tests, we investigated salient ASD features in different cell-type-specific genetic mouse models.

Results

Generation and Characterization of *Eif4ebp2*$^{flx/flx}$ Mice. To examine the cell-type-specific role of 4E-BP2 in autism-related behaviors, we deleted *Eif4ebp2* in excitatory and inhibitory neurons as well as in astrocytes. We generated *Eif4ebp2* "floxed" mice (*Eif4ebp2*$^{flx/flx}$) in which exon 2 of *Eif4ebp2* can be excised by Cre recombinase (Fig. 1*A*). PCR confirmed the insertion of *lox P* sites flanking *Eif4ebp2* exon 2 in *Eif4ebp2*$^{flx/flx}$ mice (Fig. 1*B*). To ensure that the presence of *lox P* sites did not alter the behavior of *Eif4ebp2*$^{flx/flx}$ mice, we compared them to *Eif4ebp2*$^{+/+}$ (wild type) littermates in a battery of tests that include repetitive stereotypic, social, vocal communication, anxiety, and locomotion behaviors.

To examine repetitive stereotypic behaviors, we measured total time spent grooming and the number of grooming bouts during a self-grooming assay. Both measures were similar between *Eif4ebp2*$^{flx/flx}$ and wild-type mice [Fig. 1*C*; time grooming, *Eif4ebp2*$^{flx/flx}$ 26.0 s ± 4.0 and wild type 30.2 s ± 4.6, t (21) = 0.6874, P = 0.4993; number of bouts, *Eif4ebp2*$^{flx/flx}$ 2.9 ± 0.18 and wild type 2.9 ± 0.18, t (21) = 0.08989, P = 0.9292; unpaired t test for both measures]. Similarly, *Eif4ebp2*$^{flx/flx}$ mice buried an equal number of marbles to wild-type mice [Fig. 1*D*; *Eif4ebp2*$^{flx/flx}$ 6.2 ± 0.74 and wild type 6.9 ± 0.91, t (21) = 0.5742, P = 0.5719; unpaired t test] also indicating no impairments in repetitive stereotypic behaviors in *Eif4ebp2*$^{flx/flx}$ mice.

In the 3-chamber social interaction test, wild-type and *Eif4ebp2*$^{flx/flx}$ mice exhibited robust social approach behavior, indicating a preference for sniffing stranger 1 (S1) over an empty (E) wire cage [Fig. 1 *E*, *Left*; main effect of chamber, F(1,21) = 23.36, P < 0.0001, Bonferroni's post hoc: *Eif4ebp2*$^{flx/flx}$, S1 85.2 s ± 6.9 vs. E 46.4 s ± 4.3, t (21) = 3.724, P = 0.0025 and wild type S1 88.1 s ± 7.6 vs. E 50.2 s ± 7.9, t (21) = 3.162, P = 0.0094; no main effect of genotype, F(1,21) = 0.4650, P = 0.5021; no chamber by genotype interaction, F(1,21) = 0.006141, P = 0.9383; 2-way ANOVA]. Social novelty behavior of *Eif4ebp2*$^{flx/flx}$ and wild-type mice did not differ, as both genotypes sniffed stranger 2 (S2) more than the S1 mouse [Fig. 1 *E*, *Right*; main effect of chamber, F(1,21) = 22.77, P = 0.0001, Bonferroni's post hoc: *Eif4ebp2*$^{flx/flx}$ S1 44.7 s ± 4.1 vs. S2 77.4 s ± 6.2, t (21) = 3.661, P = 0.0029 and in wild-type S1 43.8 s ± 4.0 vs. S2 75.8 s ± 8.4, t (21) = 3.137, P = 0.0100; no main effect of genotype, F(1,21) = 0.06973, P = 0.7943; no chamber by genotype interaction effect, F(1,21) = 0.003068, P = 0.9564; 2-way ANOVA].

During maternal separation, *Eif4ebp2*$^{flx/flx}$ and wild-type pups vocalized with equal call frequency [Fig. 1 *F*, *Left*; *Eif4ebp2*$^{flx/flx}$ 29.2 calls/min ± 11.4 and wild type 27.2 calls/min ± 8.2, t (10) = 0.1375, P = 0.8934; unpaired t test] and each vocalization event was similar in length between genotypes [Fig. 1 *F*, *Right*; *Eif4ebp2*$^{flx/flx}$ 13.3 ms ± 1.7 and wild type 17.0 ms ± 2.8, t (10) = 1.162, P = 0.2723; unpaired t test], indicating normal communication abilities. Since sex has no effect on mouse vocalizations at P7 in the protocol used (27), all USVs were performed with a mix of male and female mice.

When exposed to a brightly lit open arena, *Eif4ebp2*$^{flx/flx}$ and wild-type mice spent equal time in the exposed central compartment [Fig. 1 *G*, *Left*; *Eif4ebp2*$^{flx/flx}$ 72.0 s ± 8.9 and wild type 71.3 s ± 6.5, t (21) = 0.05606, P = 0.9558; unpaired t test] and travelled similar distances [Fig. 1 *G*, *Right*; *Eif4ebp2*$^{flx/flx}$ 4.5 m ± 0.24 and wild type 4.4 m ± 0.33, t (21) = 0.2540, P = 0.8020; unpaired t test], indicating unchanged anxiety levels and locomotion in *Eif4ebp2*$^{flx/flx}$ mice. Similarly, *Eif4ebp2*$^{flx/flx}$ mice remained on a rotating rod, that steadily increases in speed, for the same amount of time as wild-type mice [Fig. 1*H*; *Eif4ebp2*$^{flx/flx}$ 119 s ± 12.3 and wild type 116 s ± 14.6, t (21) = 0.8679, P = 0.8679; unpaired t test].

Taken together, our data indicate normal repetitive stereotyped, social, anxiety, and locomotor behavior in *Eif4ebp2*$^{flx/flx}$ mice.

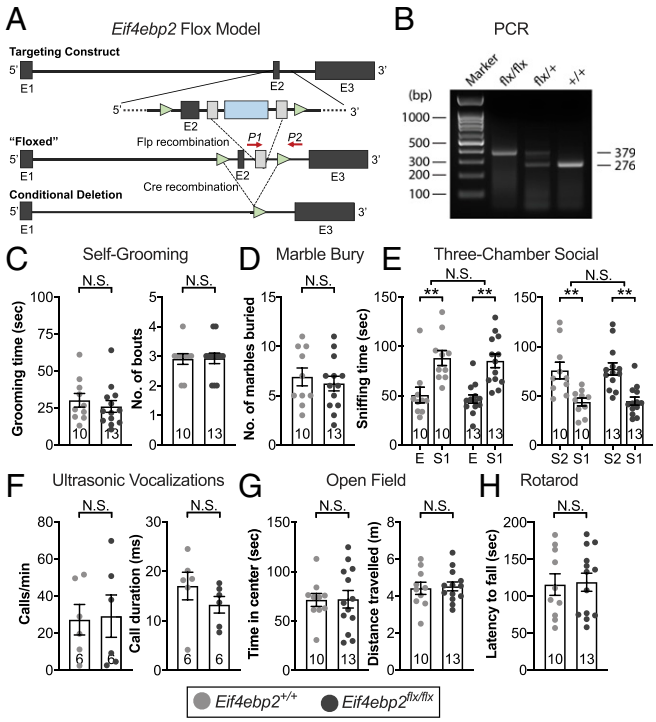

Fig. 1. Generation and characterization of *Eif4ebp2*$^{flx/flx}$ mice. (*A*) *Eif4ebp2* targeting construct design. Blue box: neomycin cassette for selection in ES cells; light-gray box: recognition sequence for FLP recombinase-mediated neo cassette removal; green arrows: recognition sequence for Cre recombinase-mediated exon deletion flanking exon 2 (E2, dark-gray box) of *Eif4ebp2*. P1 and P2 are forward and reverse primers, respectively. For the wild-type allele P1 and P2 amplify a 276-bp sequence and a 379-bp sequence in the "floxed" allele. (*B*) Confirmation of *Eif4ebp2* floxed and wild-type alleles by PCR. (*C*) Self-grooming time, number of bouts, and (*D*) number of marbles buried indicate normal repetitive stereotyped behaviors in *Eif4ebp2*$^{flx/flx}$ mice. (*E*) Social approach and novelty behaviors are unaltered in *Eif4ebp2*$^{flx/flx}$ mice in the 3-chamber social interaction test. (*F*) Analysis of the number and duration of ultrasonic vocalizations revealed normal communication in *Eif4ebp2*$^{flx/flx}$ pups. (*G*) *Eif4ebp2*$^{flx/flx}$ mice subjected to an open field analysis to investigate locomotion impairments and anxiety-driven avoidance of the center display similar behavior to control mice. (*H*) *Eif4ebp2*$^{flx/flx}$ remained on the rotating rod for the same amount of time as wild-type mice. Wild type, n = 10 and *Eif4ebp2*$^{flx/flx}$, n = 13 for all tests except ultrasonic vocalizations, where n = 6 per group. Data are displayed as mean ± SE. **P < 0.01; P > 0.05, N.S., not significant.

Deletion of *Eif4ebp2* in Excitatory Forebrain Neurons Does Not Result in Autism-Related Deficits. Calcium/calmodulin-dependent protein kinase type II alpha chain (CaMKIIα) protein is expressed in all excitatory forebrain neurons (28). To study the contribution of 4E-BP2 in excitatory neurons to autism-related deficits, we deleted 4E-BP2 in CaMKIIα-positive (+) cells. We generated *Eif4ebp2*$^{flx/flx}$*:Camk2a-Cre* and *Eif4ebp2*$^{+/+}$*:Camk2a-Cre* mice (herein, cKO-*Camk2a* and Ctl-*Camk2a*, respectively) and confirmed the lack of 4E-BP2 expression in CaMKIIα+ CA1 pyramidal neurons of the cKO-*Camk2a* hippocampus using immunofluorescence (Fig. 2*A*). Western blot analysis also revealed reduced expression of 4E-BP2 in the cKO-*Camk2a* hippocampus at postnatal day (P) 14 and 60 (29) (Fig. 2*B*).

Repetitive stereotypic behaviors were unaltered in cKO-*Camk2a* mice. We found no difference in grooming time [Fig. 2 *C*, *Left*; cKO 31.3 s ± 4.1 and Ctl 41.0 s ± 6.7, t (23) = 1.289, P = 0.2102; unpaired t test], the number of grooming bouts [Fig. 2 *C*, *Right*; cKO 3.4 ± 0.23

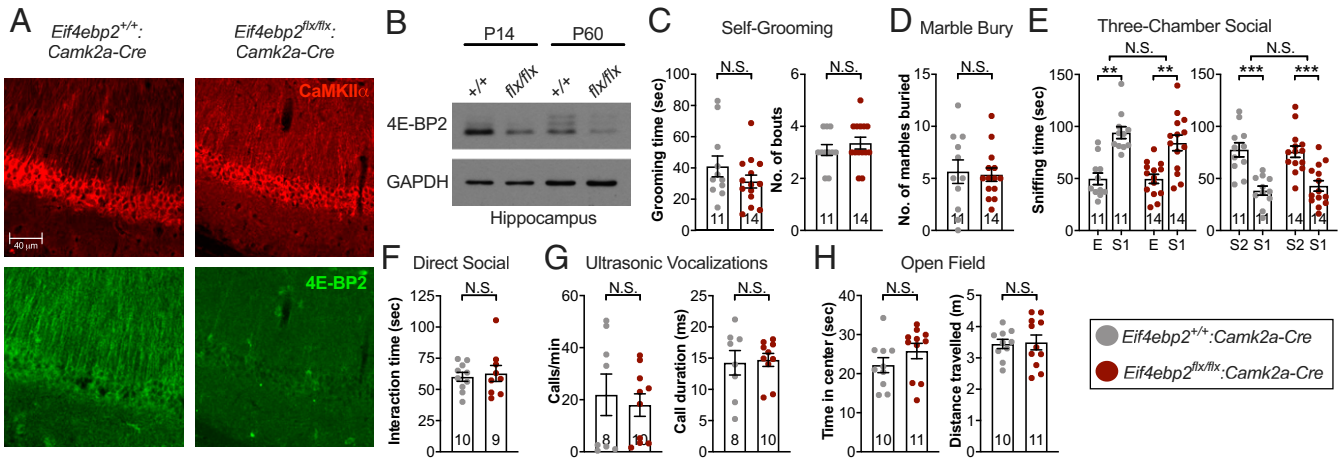

Fig. 2. Mice lacking *Eif4ebp2* in CaMKIIα+ excitatory neurons displayed normal repetitive stereotyped, social, and communication behaviors. (*A*) CaMKIIα+ hippocampal neurons express 4E-BP2 in *Eif4ebp2*$^{+/+}$*:Camk2a-Cre* (Ctl-*Camk2a*) mice but not in *Eif4ebp2*$^{flx/flx}$*:Camk2a-Cre* (cKO-*Camk2a*) mice, confirming 4E-BP2 deletion in excitatory neurons. (*B*) Immunoblot of hippocampal lysates from cKO-*Camk2a* hippocampus revealed reduced 4E-BP2 levels at P14 and P60. *A* and *B* are representative of replicated independent experiments. Measuring (*C*) self-grooming time, number of bouts, and (*D*) number of marbles buried indicated similar repetitive stereotyped behaviors in cKO-*Camk2a* ($n = 11$) and Ctl-*Camk2a* ($n = 14$) mice. (*E*) cKO-*Camk2a* ($n = 11$) and Ctl-*Camk2a* ($n = 14$) mice exposed to the 3-chamber social interaction task displayed robust social approach and novelty behaviors. (*F*) During the direct social interaction test, cKO-*Camk2a* ($n = 10$) and Ctl-*Camk2a* ($n = 9$) mice spent equal time interacting with a novel conspecific wild-type mouse. (*G*) Pup ultrasonic vocalizations were unaltered in cKO-*Camk2a* mice ($n = 10$), as compared to Ctl-*Camk2a* ($n = 8$). (*H*) Open field analysis revealed equal time in the brightly lit center chamber and distance travelled between cKO-*Camk2a* ($n = 10$) and Ctl-*Camk2a* ($n = 11$) mice. Data are displayed as mean ± SE. ***$P < 0.001$; **$P < 0.01$; $P > 0.05$, N.S., not significant.

and Ctl 3.1 ± 0.21, t (23) = 0.8432, $P = 0.4078$; unpaired t test], or the number of marbles buried [Fig. 2*D*; cKO 5.4 ± 0.64 and Ctl 5.6 ± 1.1, t (23) = 0.2263, $P = 0.8230$; unpaired t test] by cKO-*Camk2a* and Ctl-*Camk2a* mice.

In the 3-chamber social interaction test, both cKO-*Camk2a* and Ctl-*Camk2a* mice spent a longer time sniffing S1 over empty [Fig. 2 *E*, *Left*; main effect of chamber, $F(1,23) = 28.90$, $P < 0.0001$, Bonferroni's post hoc: cKO, S1 84.2 s ± 7.4 vs. E 49.7 s ± 4.4, t (23) = 3.544, $P = 0.0035$ and Ctl, S1 94.1 s ± 5.7 vs. E 49.7 s ± 5.6, t (23) = 4.042, $P = 0.0010$; no main effect of genotype, $F(1,23) = 1.328$, $P = 0.2610$; no chamber by genotype interaction effect, $F(1,23) = 0.4548$, $P = 0.5068$; 2-way ANOVA] and S2 over S1 [Fig. 2 *E*, *Right*; main effect of chamber, $F(1,23) = 35.28$, $P < 0.0001$, Bonferroni's post hoc: cKO, S1 42.8 s ± 5.1 vs. S2 75.7 s ± 5.5 t (23) = 4.076, $P = 0.0009$ and Ctl, S1 38.3 s ± 4.3 vs. *S2* 77.6 s ± 6.8, t (23) = 4.325, $P = 0.0005$; no main effect of genotype, $F(1,23) = 0.07213$, $P = 0.7907$; no chamber by genotype interaction effect, $F(1,23) = 0.2839$, $P = 0.5993$; 2-way ANOVA]. To further evaluate social behavior, we exposed cKO-*Camk2a* and Ctl-*Camk2a* mice to a novel age- and sex-matched wild-type mouse and measured the extent of direct social interaction. cKO-*Camk2a* mice spent a similar amount of time interacting with a novel mouse as compared to control animals [Fig. 2*F*; cKO 62.8 s ± 6.4 and Ctl 60.1 s ± 3.6, t (17) = 0.3764, $P = 0.7113$; unpaired t test]. Together, these data indicate that cKO-*Camk2a* mice display normal social behavior.

When separated from their mothers, cKO-*Camk2a* and Ctl-*Camk2a* pups vocalized with equal calls per minute [Fig. 2 *G*, *Left*; cKO 18.0 calls/min ± 4.3 and Ctl 21.9 calls/min ± 8.0, t(9.496) = 1.195, $P = 0.2612$; Welch's corrected (corr.) unpaired t test] and with similar length of each call [Fig. 2 *G*, *Right*; cKO 14.7 ms ± 1.0 and Ctl 14.3 ms ± 2.0, t (13) = 0.1005, $P = 0.9215$; unpaired t test], indicating unaltered communication abilities.

To test for generalized anxiety and locomotion, we exposed cKO-*Camk2a* and control mice to a brightly lit open arena. There was no difference in the amount of time spent in the center of the arena [Fig. 2 *H*, *Left*; cKO 25.8 s ± 2.0 and Ctl 22.2 s ± 1.9, t (21) = 0.05606, $P = 0.9558$; unpaired t test] nor in the overall distance moved [Fig. 2 *H*, *Right*; cKO 3.5 m ± 0.24 and Ctl 3.5 m ± 0.15, t (21) = 0.2540, $P = 0.8020$; unpaired t test] between groups.

These data show that cKO-*Camk2a* mice do not display autism-related repetitive stereotyped, social, or communication deficits.

Deletion of *Eif4ebp2* in Inhibitory Interneurons Results in Autism-Related Social Approach and Communication Deficits. Changes to the function of γ-aminobutyric (GABA) secreting interneurons has been linked to autism-related behaviors in mouse models of altered protein synthesis mechanisms (30, 31). To determine whether 4E-BP2 plays a role in autism-like behaviors via inhibitory interneurons, we deleted *Eif4ebp2* in glutamic acid decarboxylase 2 (*Gad2*)-positive cells (32). We generated *Eif4ebp2*$^{flx/flx}$*:Gad2-Cre* (cKO-*Gad2*) and *Eif4ebp2*$^{+/+}$*:Gad2-Cre* (Ctl-*Gad2*) mice and costained for 4E-BP2 and GAD67 in hippocampal slices from both genotypes to confirm deletion of 4E-BP2 in GAD67+ interneurons in cKO-*Gad2* mice (Fig. 3*A*). The GAD67 antibody also stained CA1 pyramidal neurons non-specifically as reported in another study (33). We did not observe reduced 4E-BP2 levels in cKO-*Gad2* hippocampus lysates via Western blot analysis (Fig. 3 *B*, *Upper*). However, Western blotting of proteins from cKO-*Gad2* olfactory bulbs, where *Gad2*-driven Cre recombinase activity is enriched (32), revealed reduced levels of 4E-BP2 at P14 and P60 (Fig. 3 *B*, *Lower*), consistent with the results from hippocampal immunofluorescence.

In the self-grooming assay, we observed no difference in the time spent grooming [Fig. 3 *C*, *Left*; cKO 24.1 s ± 3.9 and Ctl 37.6 s ± 8.7, t(12.67) = 1.425, $P = 0.1784$ Welch's corr. unpaired t test] or the number of bouts [Fig. 3 *C*, *Right*; cKO 5.9 ± 0.84 and Ctl 8.0 ± 1.1, t (22) = 1.568, $P = 0.1312$; unpaired t test] by cKO-*Gad2* and Ctl-*Gad2* mice. Similarly, cKO-*Gad2* mice buried the same number of marbles as control mice [Fig. 3*D*; cKO 3.8 ± 0.65 and Ctl 2.9 ± 0.48, t (22) = 1.017, $P = 0.3200$; unpaired t test], indicating normal repetitive stereotypic behaviors in these mice.

Ctl-*Gad2* mice preferred interacting with S1 to a greater extent than empty, but in contrast, cKO-*Gad2* mice did not show this preference [Fig. 3 *E*, *Left*; chamber by genotype interaction effect, $F(1,30) = 8.624$, $P = 0.0063$, Bonferroni's post hoc: cKO,

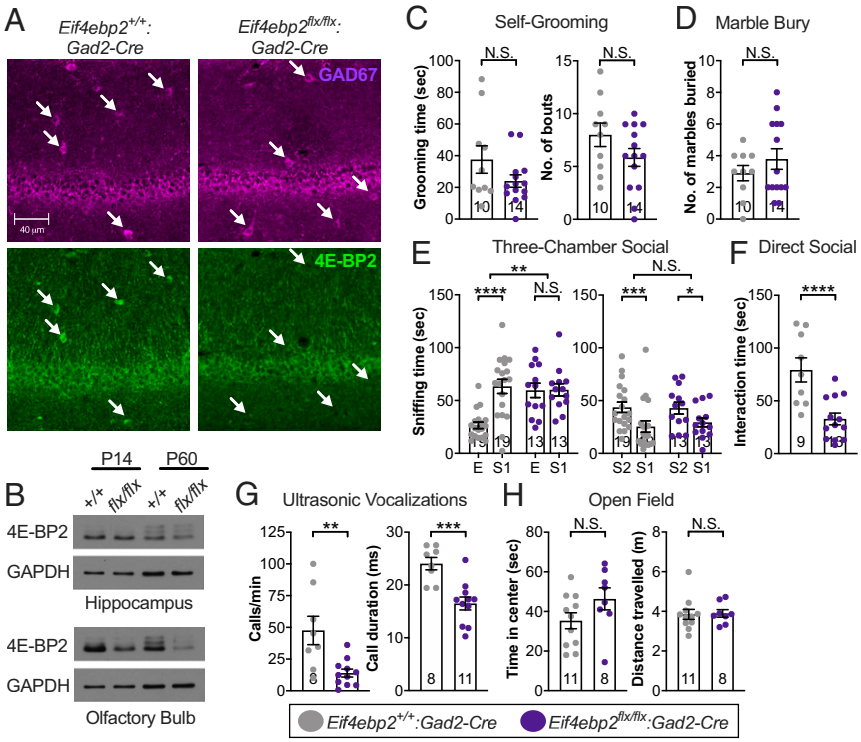

Fig. 3. Deletion of *Eif4ebp2 in* GAD67+ interneurons resulted in social approach and communication deficits. (*A*) GAD67+ interneurons express 4E-BP2 in *Eif4ebp2*$^{+/+}$*:Gad2-Cre* (Ctl-*Gad2*) mice but not in *Eif4ebp2*$^{flx/flx}$*:Gad2-Cre* (cKO-*Gad2*) mice, confirming 4E-BP2 deletion in GABAergic neurons. (*B*) Immunoblot of olfactory bulb but not hippocampal lysates from cKO-*Gad2* mice revealed reduced 4E-BP2 levels at P14 and P60. *A* and *B* are representative of replicated independent experiments. Measuring (*C*) self-grooming time, number of bouts, and (*D*) number of marbles buried indicated similar repetitive stereotypic behaviors between cKO-*Gad2* ($n = 14$) and Ctl-*Gad2* ($n = 10$) mice. (*E*) cKO-*Gad2* ($n = 13$) mice exhibited impaired social approach but normal social novelty behaviors compared to Ctl-*Gad2* ($n = 19$) mice in the 3-chamber social interaction test. (*F*) Time spent directly interacting with a conspecific adult male mouse was decreased in cKO-*Gad2* ($n = 13$) compared to Ctl-*Gad2* ($n = 9$) mice. (*G*) Maternally separated cKO-*Gad2* ($n = 11$) pups displayed decreased number and duration of ultrasonic vocalizations in comparison to Ctl-*Gad2* ($n = 8$) pups. (*H*) Time in center and distance travelled in the open field were not different between cKO-*Gad2* ($n = 8$) and Ctl-*Gad2* ($n = 11$) mice. Data are displayed as mean ± SE. ****$P < 0.0001$; ***$P < 0.001$; **$P < 0.01$; *$P < 0.05$; $P > 0.05$, N.S., not significant.

S1 60.1 s ± 5.8 vs. E 59.6 s ± 6.8, t (30) = 0.04905, $P > 0.9999$ and Ctl, S1 63.4 s ± 6.7 vs. E 26.4 s ± 3.0, t (30) = 4.667, $P = 0.0001$; main effect of chamber, $F(1,30) = 9.074$, $P = 0.0052$; main effect of genotype, $F(1,30) = 7.994$, $P = 0.0083$; 2-way ANOVA]. Both cKO-*Gad2* and Ctl-*Gad2* mice demonstrated social novelty [Fig. 3 *E*, *Right*; main effect of chamber, $F(1,30) = 19.56$, $P = 0.0001$, Bonferroni's post hoc: cKO, S1 29.5 s ± 4.3 vs. S2 42.9 s ± 5.6, t (30) = 2.441, $P = 0.0415$ and Ctl, *S1* 25.5 s ± 5.4 vs. *S2* 43.7 s ± 5.0, t (30) = 3.986, $P = 0.0008$; no main effect of genotype, $F(1,30) = 0.05985$, $P = 0.8084$; no chamber by genotype interaction effect, $F(1,30) = 0.4351$, $P = 0.5145$; 2-way ANOVA]. We then directly exposed cKO-*Gad2* and Ctl-*Gad2* mice to a wild-type mouse and measured the amount of direct social interaction. cKO-*Gad2* mice spent significantly less time interacting with a novel mouse as compared to control animals [Fig. 3*F*; cKO 32.9 s ± 5.6 and Ctl 79.3 s ± 11.4, t (20) = 4.015, $P = 0.0007$; unpaired t test].

To study vocal communication, we separated cKO-*Gad2* and control pups from their mothers, inducing ultrasonic vocalizations. cKO-*Gad2* vocalized less frequently [Fig. 3 *G*, *Left*; cKO 14.0 calls/min ± 3.1 and Ctl 47.5 calls/min ± 11.2, t (17) = 3.293, $P = 0.0043$; Welch's corr. unpaired t test] and with a shorter call duration [Fig. 3 *G*, *Right*; cKO 16.5 ms ± 1.2 and Ctl 24.1 ms ± 1.2, t (17) = 4.318, $P = 0.0005$; unpaired t test] relative to Ctl-*Gad2* pups.

To ensure that there was no effect of 4E-BP2 deletion on generalized anxiety or locomotion behavior, we exposed cKO-*Gad2* and Ctl-*Gad2* mice to a brightly lit open arena. There was no difference in the amount of time cKO-*Gad2* and controls spent in the central chamber of the arena [Fig. 3 *H*, *Left*; cKO 46.4 s ± 5.6 and Ctl 35.3 s ± 4.0, t (17) = 1.653, $P = 0.1167$; unpaired t test] or the distance travelled during the test [Fig. 3 *H*, *Right*; cKO 3.9 m ± 0.19 and Ctl 3.8 m ± 0.25, t (17) = 0.1393, $P = 0.8908$; unpaired t test].

These data reveal that mice lacking 4E-BP2 in *Gad2* interneurons are impaired in social interaction and vocal communication.

Deletion of *Eif4ebp2* in Astrocytes Does Not Cause Autism-Related Deficits. Astrocytes control excitatory and inhibitory synapse formation and morphology (25, 26). Increasing evidence indicates that astrocytic dysfunction contributes to the development of ASD (34). To examine the contribution of astrocytic 4E-BP2 to autism-specific behaviors, we deleted *Eif4ebp2* in glial fibrillary acidic protein (GFAP)-expressing astrocytes. We first generated *Eif4ebp2*$^{flx/flx}$*:Gfap-Cre* and *Eif4ebp2*$^{+/+}$*:Gfap-Cre* mice (herein, cKO-*Gfap* and Ctl-*Gfap*, respectively). Immunofluorescence confirmed 4E-BP2 deletion in GFAP+ cells from cKO-*Gfap* hippocampal slices (Fig. 4*A*). Western blot analysis revealed reduced 4E-BP2 expression in cKO-*Gfap* hippocampus lysates at P14 and P60 (Fig. 4*B*).

The total time grooming [Fig. 4 *C*, *Left*; cKO 64.3 s ± 11.9 and Ctl 86.9 s ± 12.5, t (23) = 1.277, $P = 0.2143$; unpaired t test], the amount of grooming bouts [Fig. 4 *C*, *Right*; cKO 3.6 ± 0.24 and Ctl 3.2 ± 0.35, t (23) = 0.9345, $P = 0.3598$; unpaired t test], and the number of marbles buried [Fig. 4*D*; cKO 1.4 ± 0.47 and Ctl

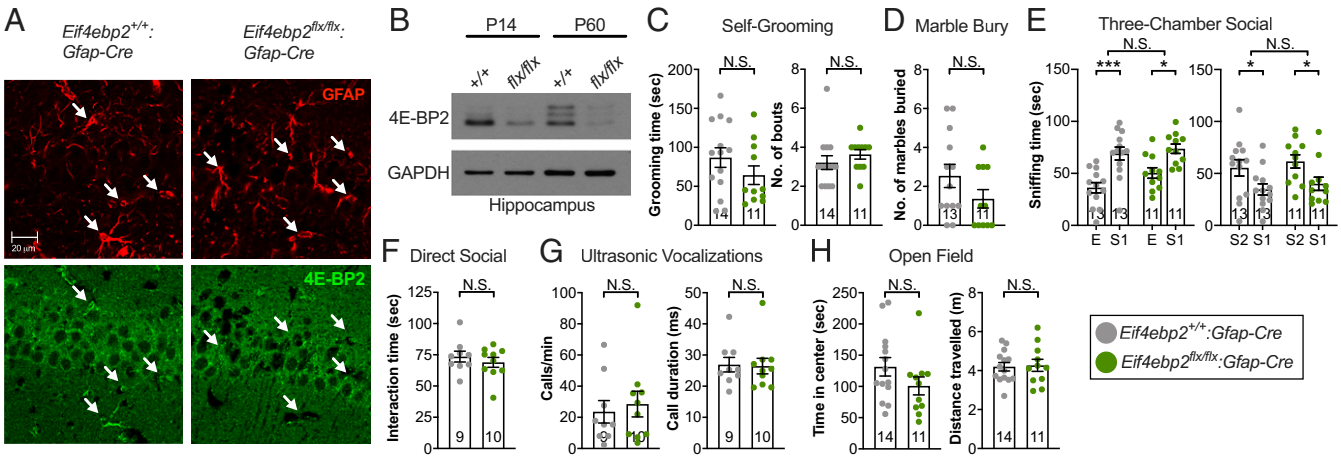

Fig. 4. Mice lacking *Eif4ebp2* in GFAP+ astrocytes displayed normal behavior. Measuring (*A*) lack of 4E-BP2 expression in GFAP+ astrocytes was confirmed in *Eif4ebp2*$^{flx/flx}$*:Gfap-Cre* (cKO-*Gfap*) mice, whereas *Eif4ebp2*$^{+/+}$*:Gfap-Cre* (Ctl-*Gfap*) mice expressed astrocytic 4E-BP2. (*B*) Immunoblot of hippocampal lysates from cKO-*Gfap* hippocampus revealed reduced 4E-BP2 levels at P14 and P60. *A* and *B* are representative of replicated independent experiments. Measuring (*C*) self-grooming time and number of grooming bouts revealed normal repetitive stereotyped behaviors in cKO-*Gfap* ($n = 11$) and Ctl-*Gfap* ($n = 14$). (*D*) Number of marbles buried also indicated similar repetitive stereotyped behaviors in cKO-*Gfap* ($n = 11$) and Ctl-*Gfap* ($n = 13$) mice. (*E*) cKO-*Gfap* ($n = 11$) and Ctl-*Gfap* ($n = 13$) mice exposed to the 3-chamber social interaction test displayed normal social approach and novelty behaviors. (*F*) In the direct social interaction test, cKO-*Gfap* ($n = 9$) and Ctl-*Gfap* ($n = 10$) mice spent equal time interacting with a novel conspecific wild-type mouse. (*G*) Maternally separated cKO-*Gfap* ($n = 10$) pups displayed the same number and duration of ultrasonic vocalizations in comparison to Ctl-*Gfap* ($n = 9$) pups. (*H*) Time in center and distance travelled in the open field were not different between cKO-*Gfap* ($n = 11$) and Ctl-*Gfap* ($n = 14$) mice. Data are displayed as mean ± SE. ***$P < 0.001$; *$P < 0.05$; $P > 0.05$, N.S., not significant.

2.5 ± 0.60, t (22) = 1.506, $P = 0.1463$; unpaired t test] was equal between Ctl-*Gfap* mice and cKO-*Gfap*.

When given a choice, cKO-*Gfap* and Ctl-*Gfap* mice showed increased sniffing of S1 over empty [Fig. 4 *E*, *Left*; main effect of chamber, $F(1,22) = 26.34$, $P < 0.0001$, Bonferroni's post hoc: cKO, S1 73.7 s ± 4.5 vs. E 50.4 s ± 5.1, t (22) = 2.898, $P = 0.0167$ and Ctl, S1 69.0 s ± 6.2 vs. E 36.2 s ± 4.9, t (22) = 4.430, $P = 0.0004$; no main effect of genotype, $F(1,22) = 3.326$, $P = 0.0818$; no chamber by genotype interaction effect, $F(1,22) = 0.7515$, $P = 0.3953$; 2-way ANOVA] and S2 over S1 [Fig. 4 *E*, *Right*; main effect of chamber, $F(1,22) = 12.97$, $P = 0.0016$, Bonferroni's post hoc: cKO, S1 40.0 s ± 6.4 vs. S2 61.6 s ± 6.4, t (22) = 2.494, $P = 0.0408$ and Ctl, S1 34.6 s ± 5.3 vs. S2 55.3 s ± 7.9, t (22) = 2.607, $P = 0.0319$; no main effect of genotype, $F(1,22) = 0.6485$, $P = 0.4293$; no chamber by genotype interaction effect, $F(1,22) = 0.0050$, $P = 0.9445$; 2-way ANOVA]. Similarly, when cKO-*Gfap* mice were directly exposed to a novel wild-type mouse, they spent equal time interacting with the stranger mouse as compared to controls [Fig. 4*F*; cKO 68.9 s ± 4.0 and Ctl 73.6 s ± 4.3, t (17) = 0.7912, $P = 0.4397$; unpaired t test]. Together, these data indicate that cKO-*Gfap* mice display normal social behavior.

cKO-*Gfap* pups separated from their mothers vocalized as frequently [Fig. 4 *G*, *Left*; cKO 28.5 calls/min ± 8.3 and Ctl 23.6 calls/min ± 7.2, t (17) = 0.4439, $P = 0.6627$; unpaired t test] and with similar call duration [Fig. 4 *G*, *Right*; cKO 26.5 ms ± 2.5 and Ctl 27.0 ms ± 2.3, t (17) = 0.1326, $P = 0.8961$; unpaired t test] compared with Ctl-*Gfap* pups.

We observed normal anxiety and locomotion in the open field by cKO-*Gfap* mice. There was no difference in the amount of time between cKO-*Gfap* and controls spent in the central chamber of the arena [Fig. 4 *H*, *Left*; cKO 101 s ± 14.4 and Ctl 131 s ± 14.8, t (23) = 1.455, $P = 0.1592$; unpaired t test] or the distance travelled during the test [Fig. 4 *H*, *Right*; cKO 4.3 m ± 0.31 and Ctl 4.2 m ± 0.22, t (23) = 0.1930, $P = 0.8487$; unpaired t test].

Overall, autism-related core deficits in repetitive stereotypic, social, and communication behaviors were not observed in cKO-*Gfap* mice.

Discussion

Here, we show that deletion of 4E-BP2 in inhibitory, but not excitatory or astrocyte cells, results in impaired social interaction and reduced vocal communication, recapitulating 2 of the 3 core deficits in ASD.

Previously, we have shown that full-body deletion of 4E-BP2 in mice resulted in exaggerated repetitive stereotypic behaviors, social impairments, and communication deficits (21). The mice exhibited exaggerated excitatory and inhibitory drive in hippocampal pyramidal cells. Since excitation was more enhanced than inhibition, it was anticipated that 4E-BP2 plays an important role in excitatory neurons in causing autistic-like behaviors. However, we did not observe any behavioral phenotypes in the cKO-*Camk2a* model. Notably, the expression of Cre recombinase in *Camk2a-Cre* mice was first reported to start at P19 (35), indicating that gene deletion in excitatory neurons occurs postnatally. This finding may explain the lack of any ASD phenotypes in the cKO-*Camk2a* model. However, using the same Cre line with floxed *Fkbp1a* mice, Hoeffer and colleagues reported reduced expression of FKBP12 as early as 2 wk of age (29). Consistent with these results, we observed reduced expression of 4E-BP2 by P14 in the cKO-*Camk2a* model (Fig. 2*B*). Given this, we conclude that deletion of 4E-BP2 in excitatory forebrain neurons as early as P14 cannot account for the behavioral deficits in the 4E-BP2 global KO mouse, but earlier developmental deletion may be required to reach a definitive answer.

We confirmed interneuron-specific deletion of 4E-BP2 in the hippocampus of cKO-*Gad2* mice compared to Ctl-*Gad2* by using coimmunofluorescence with 4E-BP2 and GAD67 (Fig. 3*A*). GAD67 and GAD65 are encoded by the *Gad1* and *Gad2* genes, respectively, and are coexpressed in most brain regions (36). As opposed to GAD65, which is exclusively found in axon terminals, GAD67 is expressed throughout the cell (37) and can therefore be readily identified in interneurons by immunofluorescence. Similar to the cKO-*Camk2a* model, we also observed reduced 4E-BP2 protein levels in cKO-*Gad2* by P14 using Western blot analysis (Fig. 3*B*), although *Gad2*-dependent Cre recombinase is expected to act earlier during embryonic development (32). This

reduction was only observed in the olfactory bulbs, where *Gad2*-driven Cre recombinase activity is enriched (32). Given the relatively small number of inhibitory neurons in the hippocampus (38), a Western blot did not show the same reduction of 4E-BP2 in the cKO-*Gad2* hippocampus.

Our results demonstrate an important role for GABAergic 4E-BP2 expression in regulating social behaviors. This is not surprising, given the important function of interneurons in ASD (39) and maintenance of circuit homeostasis, which can affect both excitatory and inhibitory neuronal properties when altered (40, 41). Dysregulation of protein synthesis in inhibitory interneurons can engender social behavior deficits, like those observed in the general 4E-BP2 KO mouse (21). Mice lacking PTEN, which inhibits protein synthesis upstream of mTORC1 and 4E-BP2 (16), in interneurons display reduced social interaction similar to cKO-*Gad2* mice (Fig. 3 *E* and *F*) and increased inhibitory postsynaptic currents in the cortex (30). A subset of *Gad2* interneurons that are parvalbumin (PV)+, directly modulate excitatory network-driven impairments in autism-related social behavior (42). This was demonstrated using optogenetics to increase the excitability of glutamate neurons in the medial prefrontal cortex of free-moving mice, resulting in a lack of sociability in the 3-chamber social interaction test (42). Specifically increasing the inhibitory tone of PV+ interneurons alone was sufficient to reverse this social deficit. This is consistent with our findings, given that all subsets of *Gad2* interneurons likely lack expression of 4E-BP2 in cKO-*Gad2* mice (43).

We observed a robust communication deficit in the cKO-*Gad2* mice (Fig. 3*G*). Interestingly, deletion of TSC1, an upstream 4E-BP2 regulator, in GABAergic Purkinje cells of the mouse cerebellum, led to reduced USVs in maternally separated pups and social deficits during the 3-chamber social interaction test (44). Other studies have found communication and social deficits similar to cKO-*Gad2* mice when deleting known ASD-risk genes, such as forkhead box P2, in which mutations result in impaired Purkinje neuron function (45–47). Given that cKO-*Gad2* mice lack 4E-BP2 in all GABAergic neurons, including Purkinje neurons (48), the observed communication deficits in cKO-*Gad2* mice might be driven by these interneurons. Social and communication behaviors remain to be evaluated in mice lacking 4E-BP2 expression in Purkinje neurons. Future work is needed to further address the contribution of 4E-BP2 in subclasses of GABAergic interneurons in autism-related social and communication impairments.

None of the cKO models studied here presented with repetitive stereotypic behaviors, which are typically manifested as exaggerated self-grooming and excessive marble burying in animal models of ASD (49, 50), including the 4E-BP2 full-body KO mouse (21). The coordinated activity of multiple brain regions and neural circuits, such as the neocortex, striatum, and cerebellum are involved in regulating different aspects of self-grooming (49). However, studies in rats with mesencephalic decerebration, in which the midbrain is intact, showed a normal sequence pattern of self-grooming, demonstrating that cortical regions of the brain are not required for the generation of this sequential pattern (51). Furthermore, many studies have shown the importance of the striatum in self-grooming (52–54). In cKO-*Camk2a* mice, deletion of 4E-BP2 is restricted to glutamatergic cells of the neocortex (35). Given this restricted gene deletion, the absence of a self-grooming phenotype emphasizes the importance of the midbrain for self-grooming behavior.

Deletion of 4E-BP2 in GABAergic interneurons and astrocytes is more broad throughout the brain (55, 56) compared to the deletion in CaMKIIα+ neurons. Therefore, the absence of a grooming phenotype in our inhibitory and astrocyte cKO models cannot be explained based on brain region or cell-type specificity alone. We conclude that deletion of 4E-BP2 in inhibitory neurons or astrocytes alone is not sufficient to elicit a self-grooming phenotype. Deletion of 4E-BP2 in multiple cell populations may therefore be required to elicit this phenotype, which was observed in the full-body KO (21). Future experiments should focus on targeting 4E-BP2 in the striatum, particularly in dopamine receptor D1 and D2 striatal neurons because of their relevance to grooming behaviors in mouse models of ASD (57), to investigate repetitive stereotyped behaviors in the context of 4E-BP2.

Dysregulation of cap-dependent mRNA translation is a cause of ASD (7). We previously demonstrated that global deletion of 4E-BP2 results in exaggerated translation of neuroligins (NLGNs) 1 through 4, which alters excitatory and inhibitory synaptic functions resulting in autism-related deficits (21). NLGNs are cell-adhesion proteins that perform a variety of important synaptic functions, including signal integration and synaptic formation, and have been implicated in a number of cognitive disorders (58). Our findings in cKO-*Gad2* mice may reflect NLGN-mediated dysregulation of inhibitory synaptic activity.

Using a combination of molecular genetics and behavioral neuroscience, we provide evidence for an inhibitory interneuron-specific role of 4E-BP2 in the development of autistic-like behaviors. Understanding the basic pathophysiology of ASD-linked genes could provide a preclinical basis for more precise and targeted therapeutic interventions to reverse autism-like symptoms (59).

Materials and Methods

Generating Eif4ebp2$^{flx/flx}$ Mice. The *Eif4ebp2* conditional mouse line (Fig. 1*A*) was generated by Ozgene Pty Ltd (Bentley WA, Australia). The construct targeting exon 2 of *Eif4ebp2* was electroporated into the C57BL/6J embryonic stem (ES) cell line, Bruce4 (60). Homologous recombinant ES cell clones were identified by Southern hybridization and injected into blastocysts. Male chimeric mice were obtained and crossed to C57BL/6J females to establish heterozygous germline offspring on C57BL/6J background. Germline mice were crossed to a ubiquitous flippase (FLP) C57BL/6J mouse line to remove the FRT-flanked selectable marker cassette. The BACs used as a template for PCR to generate the fragments used to construct the targeting vector were RP23-117C21 and RP23-202I1.

Generating Eif4ebp2 Conditional Knockout Mice. To generate conditionally deleted 4E-BP2 mice, *Eif4ebp2$^{flx/flx}$* mice were crossed with wild-type mice expressing Cre recombinase under the control of different cell-type-specific promoters. The Cre-positive flx/+ heterozygous progeny were then crossed to each other to generate the following strains: *Eif4ebp2$^{+/+}$:Camk2a-Cre* and *Eif4ebp2$^{flx/flx}$:Camk2a-Cre* (glutamatergic neocortical neurons (35), JAX stock no: 005359, on C57BL/6J background); *Eif4ebp2$^{+/+}$:Gad2-Cre* and *Eif4ebp2$^{flx/flx}$:Gad2-Cre* (GABAergic interneurons (32), JAX stock no: 010802, on C57BL/6 background); and *Eif4ebp2$^{+/+}$:Gfap-Cre* and *Eif4ebp2$^{flx/flx}$:Gfap-Cre* (astrocytes (61), JAX stock no: 024098, on C57BL/6J background). To normalize for any confounding effects generated by the presence of Cre recombinase, comparisons were made between control (indicated as Ctl-*Cre*) and cKO-*Cre* mice. Parallel experiments were conducted on *Eif4ebp2$^{+/+}$* versus *Eif4ebp2$^{flx/flx}$* mice without Cre expression to control for any effects generated by the insertion of *loxP* sites in the *Eif4ebp2* gene.

Mice. Adult male mice (P60–P90) were used for behavioral experiments. Mouse pups (P7) of both sexes were used for ultrasonic vocalizations, since the animal sex has no effect on vocalizations at P7 with the protocol used (27). After weaning at P21, mice were group housed by sex in groups of 2 to 5 per cage with ad libitum access to food and water. Cages were maintained in ventilated racks in temperature (20 to 21 °C) and humidity (~55%) controlled rooms, on a 12 h light/dark cycle. Standard corncob bedding was used for housing (Harlan Laboratories, Inc). Adult mice were handled once per day for 2 to 3 d before behavioral testing. All behavioral experiments were conducted in an isolated sound-proof room between 7 AM and 3 PM. Before behavioral testing, mice were habituated for 30 min to the experimental room. All procedures followed the Canadian Council on Animal Care guidelines and were approved by the McGill University Animal Care Committee.

Self-Grooming. Mice were individually placed in a new cage with ~1 cm of fresh bedding material but without nesting material. Self-grooming behavior was recorded for 20 min using a high-resolution video camera placed in front of the cage. Total grooming time and the number of grooming bouts were manually scored using a stopwatch.

Marble Burying. Mice were placed individually in an open arena (51.5 cm by 51.5 cm by 31 cm) containing fresh bedding (i.e., sawdust, 5 cm deep) with 20 clean marbles prearranged in a 5 by 4 grid. Mice were allowed to bury the marbles for 20 min. After the test period, buried marbles were counted manually. Marbles were considered buried if they were at least 2/3 covered with sawdust.

Three-Chamber Social Interaction Test. A 3-chamber arena with openings between the chambers was used to assess sociability and preference for social novelty. Test mice were placed in the middle chamber and allowed to freely explore the empty 3-chamber arena for 10 min. Immediately after habituation, an unfamiliar mouse (stranger 1, male C57BL/6J age matched) was introduced into 1 of the 2 side chambers, enclosed in a wire cage allowing only the test mouse to initiate any social interaction. An identical empty wire cage was placed in the other side chamber. With this setup, the test mouse was again placed in the middle chamber and allowed to explore the 3-chamber arena for 10 min. At the end of the 10-min sociability test, a new unfamiliar mouse (stranger 2, male C57BL/6J age matched) was placed in the previously unoccupied wire cage. The test mouse was examined for an additional 10 min to assess social novelty. The location of the empty wire cage was alternated between side chambers for different test mice to prevent chamber biases. Stranger 1 and 2 mice were always taken from separate home cages and counterbalanced for each side and stranger cage. The time spent sniffing stranger 1, stranger 2, or the empty wire cage was manually scored. All stranger mice were purchased from Charles River Laboratories (Sherbrooke, QC).

Direct Social Interaction. Test mice were placed in a clean cage containing 1 cm of fresh bedding material and given 5 min to habituate. Immediately after habituation, a novel age- and sex-matched conspecific stranger mouse was introduced into the cage and the mice were able to freely engage in social interaction for 10 min. The interaction time, defined by the following behavior: nose-to-anogenital sniffing, nose-to-nose sniffing, and social grooming, was manually scored.

Isolation-Induced Ultrasonic Vocalizations. A microphone (Avisoft Bioacoustics CM16/CMPA) was fixed inside the top of an anechoic styrofoam chamber. The microphone was connected to an ultrasound recording interface (Avisoft Bioacoustics UltraSoundGate 116Hb), which detects USVs emitted by newborn mouse pups and transferred those signals to a standard PC for recording using a digital recording system (Avisoft Bioacoustics RECORDER). Newborn mouse pups (P7) were carefully separated from their mothers for 15 min to induce USVs. The newborn mouse pups were then placed individually in the recording chamber and USVs were recorded for 5 min. Recordings were analyzed manually using the Avisoft Bioacoustics SASLab Pro. The number of calls per minute and average call duration were recorded.

Open Field. Mice were placed individually in a brightly lit (1,200 lx) square arena (51.5 cm by 51.5 cm) enclosed by 31 cm high, opaque white walls without a lid. Mice were allowed to move freely for 10 min, while their locomotor activity was tracked using the Noldus EthoVision XT video tracking software. Total distance moved and time spent in the center were calculated using the tracking software.

Rotarod. The IITC Life Science Rotarod apparatus was used to assess gross motor function. Mice were individually placed on a 11/4 inch diameter rod facing away from the direction of rotation. Before testing, mice were trained to stay on the rod at a constant rotation speed of 5 revolutions per minute (rpm). Mice that repeatedly fell were placed back on the rotarod until the end of the 3-min training period. Trained mice were then tested on a gradually accelerating rotarod for 5 min. The rotation speed began at 5 rpm and accelerated by 0.2 rpm per second. The latency to fall off the rotarod was recorded.

Immunohistochemistry. Coronal hippocampal sections (20 μm) were prepared from whole brains of adult male mice (P60–P120) after transcardial perfusion fixation using PBS and then 4% paraformaldehyde (Cat. No. 101169, FD NeuroTechnologies, Inc.). Sections were blocked (1 h, room temperature) in blocking buffer composed of 10% BSA and 0.5% Tween 20 in PBS and incubated (overnight, 4 °C) in rabbit polyclonal antibody against 4E-BP2 (Cat. No. 2845S, Cell Signaling Technology) diluted 1:50 in blocking buffer, mouse monoclonal antibody against CaMKII-α (Cat. No. 50049, Cell Signaling Technology) diluted 1:1,000 in blocking buffer, or mouse monoclonal antibody against GAD67 (Cat. No. MAB5406B, EMD Millipore) diluted 1:1,000 in blocking buffer, or mouse monoclonal antibody against GFAP (Cat. No. 3670S, Cell Signaling Technology) diluted 1:100 in blocking buffer. After washing with PBS, sections were incubated in darkness (1 h, room temperature) in Alexa Fluor 488 goat anti-rabbit IgG (Cat. No. A11034, Thermo Fisher Scientific) diluted 1:300, Alexa Fluor 546 donkey anti-mouse IgG (Cat. No. A10036, Thermo Fisher Scientific) diluted 1:300 and Hoechst 33342, trihydrochloride, trihydrate (Cat. No. H3570, Life Technologies) diluted 1:1,000 in blocking buffer. Sections were then washed with PBS. Samples were visualized using a Zeiss LSM880 laser scanning confocal microscope.

Western Blotting. The hippocampus and olfactory bulbs (where indicated) were carefully dissected from male mice (P14 and P60) and homogenized in ice-cold lysis buffer (RIPA Cat. No. R0278, Sigma-Aldrich) containing 1 tablet EDTA-free protease inhibitor mixture (Cat. No. 469315901, cOmplete from Roche), phosphatase inhibitor mixture 2 (Cat. No. P5726, Sigma-Aldrich) diluted 1:100, and phosphatase inhibitor mixture 3 (Cat. No. P0044, Sigma-Aldrich) diluted 1:100. A total of 25 μg of protein lysate was loaded and run on a 15% acrylamide SDS/PAGE gel and then transferred to a nitrocellulose membrane. The membrane was blocked (1 h, room temperature) in blocking buffer (5% BSA and 1% Tween 20 in TBS) and incubated overnight at 4 °C in rabbit polyclonal antibody against 4E-BP2 (Cat. No. 2845S, Cell Signaling Technology) diluted 1:500 in blocking buffer or mouse monoclonal antibody against GAPDH (Cat. No. ab9842, abcam) diluted 1:20,000 in blocking buffer. The membranes were then washed with fresh TBST (3 times, 10 min/wash) and incubated for 1 h at room temperature in horseradish peroxidase-conjugated secondary antibody (Cat. No. ab6271, abcam) diluted 1:5,000 in blocking buffer. The blots were washed with fresh TBST (3 times, 10 min/wash) and visualized on HyBlot CL autoradiography film (Cat. No. 1159M38, Thomas Scientific).

Genotyping. A standard PCR genotyping protocol was used to confirm the genotypes of all mice used in this study. DNA samples were prepared by extracting genomic DNA from mouse ear or tail samples. To genotype the *Eif4ebp2* alleles, the forward primer (5′-GTCGGTCTTCTGTAGATTGTGAGT-3′) and the reverse primer (5′-GGCGATCCCTAGAAAATAAAGCCT-3′) were used to detect the wild-type allele (276 bp) and the "floxed" allele (379 bp). To genotype Cre (~300 bp), the forward primer (5′-GATTGCTTATAACACCCTGTTACG-3′) and the reverse primer (5′-GTAAATCAATCGATGAGTTGCTTCA-3′) were used. The PCR products were visualized on an agarose gel with ethidium bromide.

Statistical Analysis and Behavioral Scoring. Experimenters were blinded to the genotype during testing and scoring. All data are presented as mean ± SEM (error bars). Statistical significance was set a priori at alpha = 0.05. Unpaired Student's *t* tests were used to calculate *P* values for all test measures except for the 3-chamber social interaction sniffing measures, where a 2-way ANOVA was used. A Welch's corrected *t* test was used in cases where the Levene test produced a significant ($P < 0.05$) difference in the variance of data between groups.

ACKNOWLEDGMENTS. For communicating with and assisting Ozgene in the initial design of the *Eif4ebp2* targeting construct we thank Christos Gkogkas (University of Edinburgh). We thank Karim Nader (McGill University) for providing access to his behavioral testing rooms. Further, we thank Jeffery Mogil (McGill University) for allowing us to house our genetic animal models in his facility. Finally, we would like to thank our animal husbandry experts, Annie Sylvestre and Annik Lafrance, for their hard work in setting up the breedings, weaning, and ear-notching of mice and their help with the initial genotyping. Funding was provided by a Brain Canada/FNC grant; a Canadian Institutes of Health Research foundation grant (FDN-148423); Howard Hughes Medical Institute Distinguished Researcher (No. 55007654); a Brain & Behaviour Research Foundation grant (to N.S.); a FRAXA Research Foundation/ Fragile X Research Foundation of Canada Fellowship (to I.G.); the Richard Tomlinson Doctoral Fellowship (to S.W.); and the Healthy Brains for Healthy Lives Fellowship (Canada First Research Excellence Fund to McGill University) (to A.N.).

1. M. Elsabbagh *et al*., Global prevalence of autism and other pervasive developmental disorders. *Autism Res.* **5**, 160–179 (2012).
2. M.-C. Lai, M. V. Lombardo, S. Baron-Cohen, Autism. *Lancet* **383**, 896–910 (2014).
3. B. Devlin, S. W. Scherer, Genetic architecture in autism spectrum disorder. *Curr. Opin. Genet. Dev.* **22**, 229–237 (2012).
4. S. De Rubeis *et al*.; DDD Study; Homozygosity Mapping Collaborative for Autism; UK10K Consortium, Synaptic, transcriptional and chromatin genes disrupted in autism. *Nature* **515**, 209–215 (2014).
5. R. K. C Yuen *et al*., Whole genome sequencing resource identifies 18 new candidate genes for autism spectrum disorder. *Nat. Neurosci.* **20**, 602–611 (2017).

6. I. Iossifov *et al*., The contribution of de novo coding mutations to autism spectrum disorder. *Nature* **515**, 216–221 (2014).
7. E. Santini, E. Klann, Reciprocal signaling between translational control pathways and synaptic proteins in autism spectrum disorders. *Sci. Signal* **7**, re10 (2014).
8. D. H. Ebert, M. E. Greenberg, Activity-dependent neuronal signalling and autism spectrum disorder. *Nature* **493**, 327–337 (2013).
9. A. G. Hinnebusch, I. P. Ivanov, N. Sonenberg, Translational control by 5′-untranslated regions of eukaryotic mRNAs. *Science* **352**, 1413–1416 (2016).
10. R. E. Thach, Cap recap: The involvement of eIF-4F in regulating gene expression. *Cell* **68**, 177–180 (1992).
11. A. Pause, N. Méthot, Y. Svitkin, W. C. Merrick, N. Sonenberg, Dominant negative mutants of mammalian translation initiation factor eIF-4A define a critical role for eIF-4F in cap-dependent and cap-independent initiation of translation. *EMBO J.* **13**, 1205–1215 (1994).
12. R. Duncan, S. C. Milburn, J. W. Hershey, Regulated phosphorylation and low abundance of HeLa cell initiation factor eIF-4F suggest a role in translational control. Heat shock effects on eIF-4F. *J. Biol. Chem.* **262**, 380–388 (1987).
13. J. D. Richter, N. Sonenberg, Regulation of cap-dependent translation by eIF4E inhibitory proteins. *Nature* **433**, 477–480 (2005).
14. N. Sonenberg, A. G. Hinnebusch, Regulation of translation initiation in eukaryotes: Mechanisms and biological targets. *Cell* **136**, 731–745 (2009).
15. A. C. Gingras *et al*., Regulation of 4E-BP1 phosphorylation: A novel two-step mechanism. *Genes Dev.* **13**, 1422–1437 (1999).
16. C.-H. Kwon *et al*., Pten regulates neuronal arborization and social interaction in mice. *Neuron* **50**, 377–388 (2006).
17. K. M. Huber, E. Klann, M. Costa-Mattioli, R. S. Zukin, Dysregulation of mammalian target of rapamycin signaling in mouse models of autism. *J. Neurosci.* **35**, 13836–13842 (2015).
18. M. Costa-Mattioli, L. M. Monteggia, mTOR complexes in neurodevelopmental and neuropsychiatric disorders. *Nat. Neurosci.* **16**, 1537–1543 (2013).
19. E. Rosina *et al*., Disruption of mTOR and MAPK pathways correlates with severity in idiopathic autism. *Transl. Psychiatry* **9**, 50 (2019).
20. M. V. Lombardo *et al*., Maternal immune activation dysregulation of the fetal brain transcriptome and relevance to the pathophysiology of autism spectrum disorder. *Mol. Psychiatry* **23**, 1001–1013 (2018).
21. C. G. Gkogkas *et al*., Autism-related deficits via dysregulated eIF4E-dependent translational control. *Nature* **493**, 371–377 (2013).
22. E. Santini *et al*., Exaggerated translation causes synaptic and behavioural aberrations associated with autism. *Nature* **493**, 411–415 (2013).
23. M. Neves-Pereira *et al*., Deregulation of EIF4E: A novel mechanism for autism. *J. Med. Genet.* **46**, 759–765 (2009).
24. J. L. Banko *et al*., The translation repressor 4E-BP2 is critical for eIF4F complex formation, synaptic plasticity, and memory in the hippocampus. *J. Neurosci.* **25**, 9581–9590 (2005).
25. G. Perea, M. Navarrete, A. Araque, Tripartite synapses: Astrocytes process and control synaptic information. *Trends Neurosci.* **32**, 421–431 (2009).
26. J. A. Stogsdill *et al*., Astrocytic neuroligins control astrocyte morphogenesis and synaptogenesis. *Nature* **551**, 192–197 (2017).
27. X. Yin *et al*., Maternal deprivation influences pup ultrasonic vocalizations of C57BL/6J mice. *PLoS One* **11**, e0160409 (2016).
28. K. M. Jacobs, R. L. Neve, J. P. Donoghue, Neocortex and hippocampus contain distinct distributions of calcium-calmodulin protein kinase II and GAP43 mRNA. *J. Comp. Neurol.* **336**, 151–160 (1993).
29. C. A. Hoeffer *et al*., Removal of FKBP12 enhances mTOR-Raptor interactions, LTP, memory, and perseverative/repetitive behavior. *Neuron* **60**, 832–845 (2008).
30. D. Vogt, K. K. A. Cho, A. T. Lee, V. S. Sohal, J. L. R. Rubenstein, The parvalbumin/somatostatin ratio is increased in Pten mutant mice and by human PTEN ASD alleles. *Cell Rep.* **11**, 944–956 (2015).
31. C. Fu *et al*., GABAergic interneuron development and function is modulated by the Tsc1 gene. *Cereb. Cortex* **22**, 2111–2119 (2012).
32. H. Taniguchi *et al*., A resource of Cre driver lines for genetic targeting of GABAergic neurons in cerebral cortex. *Neuron* **71**, 995–1013 (2011). Erratum in: *Neuron* **72**, 1091 (2011).
33. T. Uchida, T. Furukawa, S. Iwata, Y. Yanagawa, A. Fukuda, Selective loss of parvalbumin-positive GABAergic interneurons in the cerebral cortex of maternally stressed Gad1-heterozygous mouse offspring. *Transl. Psychiatry* **4**, e371 (2014).
34. F. Petrelli, L. Pucci, P. Bezzi, Astrocytes and microglia and their potential link with autism spectrum disorders. *Front. Cell. Neurosci.* **10**, 21 (2016).
35. J. Z. Tsien *et al*., Subregion- and cell type-restricted gene knockout in mouse brain. *Cell* **87**, 1317–1326 (1996).
36. J. J. Soghomonian, D. L. Martin, Two isoforms of glutamate decarboxylase: Why? *Trends Pharmacol. Sci.* **19**, 500–505 (1998).
37. D. L. Kaufman, C. R. Houser, A. J. Tobin, Two forms of the gamma-aminobutyric acid synthetic enzyme glutamate decarboxylase have distinct intraneuronal distributions and cofactor interactions. *J. Neurochem.* **56**, 720–723 (1991).
38. M. J. Bezaire, I. Soltesz, Quantitative assessment of CA1 local circuits: Knowledge base for interneuron-pyramidal cell connectivity. *Hippocampus* **23**, 751–785 (2013).
39. J. W. Lunden, M. Durens, A. W. Phillips, M. W. Nestor, Cortical interneuron function in autism spectrum condition. *Pediatr. Res.* **85**, 146–154 (2019).
40. N. Dehorter, N. Marichal, O. Marín, B. Berninger, Tuning neural circuits by turning the interneuron knob. *Curr. Opin. Neurobiol.* **42**, 144–151 (2017).
41. E. Castillo-Gómez, M. Pérez-Rando, S. Vidueira, J. Nacher, Polysialic acid acute depletion induces structural plasticity in interneurons and impairs the excitation/inhibition balance in medial prefrontal cortex organotypic cultures. *Front. Cell. Neurosci.* **10**, 170 (2016).
42. O. Yizhar *et al*., Neocortical excitation/inhibition balance in information processing and social dysfunction. *Nature* **477**, 171–178 (2011).
43. B. Rudy, G. Fishell, S. Lee, J. Hjerling-Leffler, Three groups of interneurons account for nearly 100% of neocortical GABAergic neurons. *Dev. Neurobiol.* **71**, 45–61 (2011).
44. P. T. Tsai *et al*., Autistic-like behaviour and cerebellar dysfunction in Purkinje cell Tsc1 mutant mice. *Nature* **488**, 647–651 (2012).
45. E. Fujita, Y. Tanabe, B. A. Imhof, M. Y. Momoi, T. Momoi, Cadm1-expressing synapses on Purkinje cell dendrites are involved in mouse ultrasonic vocalization activity. *PLoS One* **7**, e30151 (2012).
46. Y.-H. Jiang *et al*., Altered ultrasonic vocalization and impaired learning and memory in Angelman syndrome mouse model with a large maternal deletion from Ube3a to Gabrb3. *PLoS One* **5**, e12278 (2010).
47. E. Fujita *et al*., Ultrasonic vocalization impairment of Foxp2 (R552H) knockin mice related to speech-language disorder and abnormality of Purkinje cells. *Proc. Natl. Acad. Sci. U.S.A.* **105**, 3117–3122 (2008).
48. S. Besser *et al*., A transgenic mouse line expressing the red fluorescent protein tdTomato in GABAergic neurons. *PLoS One* **10**, e0129934 (2015).
49. A. V. Kalueff *et al*., Neurobiology of rodent self-grooming and its value for translational neuroscience. *Nat. Rev. Neurosci.* **17**, 45–59 (2016).
50. E. Pasciuto *et al*., Autism spectrum disorders: Translating human deficits into mouse behavior. *Neurobiol. Learn. Mem.* **124**, 71–87 (2015).
51. K. C. Berridge, Progressive degradation of serial grooming chains by descending decerebration. *Behav. Brain Res.* **33**, 241–253 (1989).
52. D. M. Friend, A. V. Kravitz, Working together: Basal ganglia pathways in action selection. *Trends Neurosci.* **37**, 301–303 (2014).
53. J. W. Aldridge, K. C. Berridge, A. R. Rosen, Basal ganglia neural mechanisms of natural movement sequences. *Can. J. Physiol. Pharmacol.* **82**, 732–739 (2004).
54. X. Jin, F. Tecuapetla, R. M. Costa, Basal ganglia subcircuits distinctively encode the parsing and concatenation of action sequences. *Nat. Neurosci.* **17**, 423–430 (2014).
55. J. M. Tepper, F. Tecuapetla, T. Koós, O. Ibáñez-Sandoval, Heterogeneity and diversity of striatal GABAergic interneurons. *Front. Neuroanat.* **4**, 150 (2010).
56. J. R. Taft, R. P. Vertes, G. W. Perry, Distribution of GFAP+ astrocytes in adult and neonatal rat brain. *Int. J. Neurosci.* **115**, 1333–1343 (2005).
57. A. L. Bey *et al*., Brain region-specific disruption of Shank3 in mice reveals a dissociation for cortical and striatal circuits in autism-related behaviors. *Transl. Psychiatry* **8**, 94 (2018).
58. T. C. Südhof, Neuroligins and neurexins link synaptic function to cognitive disease. *Nature* **455**, 903–911 (2008).
59. S. Braat, R. F. Kooy, The GABAA receptor as a therapeutic target for neurodevelopmental disorders. *Neuron* **86**, 1119–1130 (2015).
60. F. Köntgen, G. Süss, C. Stewart, M. Steinmetz, H. Bluethmann, Targeted disruption of the MHC class II Aa gene in C57BL/6 mice. *Int. Immunol.* **5**, 957–964 (1993).
61. A. D. R. Garcia, N. B. Doan, T. Imura, T. G. Bush, M. V. Sofroniew, GFAP-expressing progenitors are the principal source of constitutive neurogenesis in adult mouse forebrain. *Nat. Neurosci.* **7**, 1233–1241 (2004).